Acta Cryst. (1999). B**55**, 341–347

Disparate atomic displacements in skutterudite-type $LaFe_3CoSb_{12}$, a model for thermoelectric behavior

Bryan C. Chakoumakos,* Brian C. Sales, David Mandrus and Veerle Keppens

Solid State Division, Oak Ridge National Laboratory, Oak Ridge, Tennessee 37831-6393, USA. E-mail: kou@ornl.gov

(*Received 20 March 1998; accepted 22 December 1998*)

Abstract

Mean-square atomic displacements in lanthanum triiron cobalt dodecaantimonide, determined as a function of temperature using single-crystal neutron diffraction, show that the La atom exhibits an anomalously large displacement at room temperature, U_{eq} = 0.0196 (9) Å^2, because it is too small to fill the atomic cage formed by the corner-linked octahedral framework of M_4Sb_{12}, M = Fe, Co. Site-occupancy refinements show 25% vacancies on the La site and an actual Fe:Co ratio of 2.17:1. Analysis of the temperature dependence of the atomic displacements identifies a significant temperature-independent component for the La atom ascribed to static disorder, which amounts to 19% of the room-temperature value. The large-amplitude rattling of the La atom can be effectively linked to the dramatic decrease of the lattice contribution to the thermal conductivity, which is a key factor for improving the thermoelectric behavior of these materials. This structure–property relationship offers a new paradigm for the exploration of thermoelectric materials.

1. Introduction

The ultimate thermoelectric material should conduct electricity like a metallic crystal, but conduct heat like a glass (Slack, 1995). Quaternary compounds, such as the title compound $LaFe_3CoSb_{12}$, meet many of the requirements for good thermoelectric materials, namely low electrical resistivity, poor thermal conductivity and a large Seebeck coefficient; their structural chemistry is being tailored to optimize the essential transport properties (Morelli & Meisner, 1995; Sales *et al.*, 1996; Mahan *et al.*, 1997; Mandrus *et al.*, 1997; Sales *et al.*, 1997). For the skutterudite structure the M_4Sb_{12} corner-linked octahedral framework (Fig. 1*a*) dominates the band structure and therefore the electronic transport. The lanthanide atoms are loosely stuffed into oversized framework cages and effectively scatter heat-carrying phonons, thereby reducing the lattice contribution to the thermal conductivity. The thermoelectric figure of merit, ZT, is near 1 at 800 K. $LaFe_4Sb_{12}$ was initially synthesized by Braun and Jeitschko and shown to have the filled skutterudite structure on the basis of single-crystal X-ray structure refinement (Braun & Jeitschko, 1980*a*). Moreover, they noted the lack of a lanthanide contraction in this and other filled skutterudite LnM_3Pn_{12} compounds, where Ln = lanthanide, M = Fe, Ru, Os and Pn = P, As, Sb (Braun & Jeitschko, 1980*b*,*c*). This suggested that the large motion of the La atom was a consequence of the atomic environment about the La atom being too large. Here, we present an analysis of the temperature dependence of the anisotropic displacement parameters in a filled skutterudite, nominally $LaFe_3CoSb_{12}$, and relate the results to the thermoelectric properties. This structure–property relationship offers a new paradigm for the exploration of thermoelectric materials. Neutron diffraction methods are advantageous in this case, not only because the nuclear scattering eliminates chemical bonding effects which often bias structural parameters refined from X-ray diffraction data, but also because absorption is insignificant and the scattering-length difference for Fe and Co allows for a good site-occupancy refinement.

2. Experimental

Polycrystalline $LaFe_3CoSb_{12}$ was prepared by melting stoichiometric quantities of high purity elements in carbon-coated, evacuated and sealed silica tubes at temperatures of 1273 to 1373 K for 24 to 48 h. The silica tubes were removed from the furnace at high temperature and quenched in a water bath. The samples were subsequently annealed at 973 K for several days. Single crystals of $La_{1-y}Fe_{3-x}Co_xSb_{12}$ were grown using the Bridgmann method with an excess of antimony and lanthanum. The as-grown 4 × 1 × 1 cm crystal boule was silver in color and exhibited a compositional gradient, being Co-rich at the bottom and Fe-rich at the top relative to the starting composition.

The neutron diffraction measurements were made at the High Flux Isotope Reactor at Oak Ridge National Laboratory. Single-crystal measurements employed the HB2a four-circle diffractometer with a Huber goniometer and a Crystal Logic controller, and utilized the 115 reflection from a Ge monochromator at a take-off angle of 45°. From this instrument configuration the neutron wavelength of 0.8387 Å was calibrated using a

crystal of KCl (a = 6.2910 Å). A parallelepipedic crystal 2.5 × 2.5 × 3.5 mm in size was sawn from the middle of the boule, glued to an aluminium pin, and mounted on the cold-tip of a closed-cycle He refrigerator, which was mounted on the diffractometer and used to control the temperature. For data collection at each temperature the same set of 31 reflections in the 2θ range 36.43–85.25° was used for refining the lattice parameter and determining the orientation matrix. The data collections were carried out by radially scanning through the Ewald sphere. At the limits of $2\theta = 0$ and 180° the radial scan is a pure ω scan and a pure θ–2θ scan, respectively; in between a simple trigonometric relationship controls the relative speeds of the ω and 2θ motors. A $\frac{1}{8}$ sphere of Bragg reflections ($0 \le h, k, l \le 16$) was measured to $\sin\theta/\lambda = 0.914$ Å^{-1}. Three intense reflections were monitored every 200 reflections to correct the intensities for variations in the neutron flux, which did not vary by more than 1% for the duration of each data collection. The reflection intensities were integrated using the Lehmann–Larson algorithm and corrected for the Lorentz effect using *REDUCE* in *UCLA Crystallographic Computing Package* (Strouse, 1994). The linear neutron attenuation factor (including both incoherent scattering and absorption) for the crystal used in this study is small, 0.0165 mm^{-1}, which gives $\mu r \simeq 0.023$. ψ scans confirmed that absorption was not significant, so an absorption correction was not applied. The scattering cross sections used throughout were taken from Sears (1992). The intensities of equivalent reflections were averaged in the cubic space group $Im\bar{3}$. About 1475 reflections were measured for each of the different data collections, leading to about 300 independent reflections with $I > 0$. The integrated intensities were used in a full-matrix least-squares refinement of the scale factor, atomic positions, and anisotropic displacement parameters (ADPs) using *GSAS* (Larson & Von Dreele, 1986) with weights $w = [2F_o/\sigma(F_o^2)]^2$. Extinction was not significant, but a Becker–Coppens type I isotropic correction was refined. In this formalism, type I means that secondary extinction is dominated by the crystal mosaic. Further experimental details are given in Table 1.†

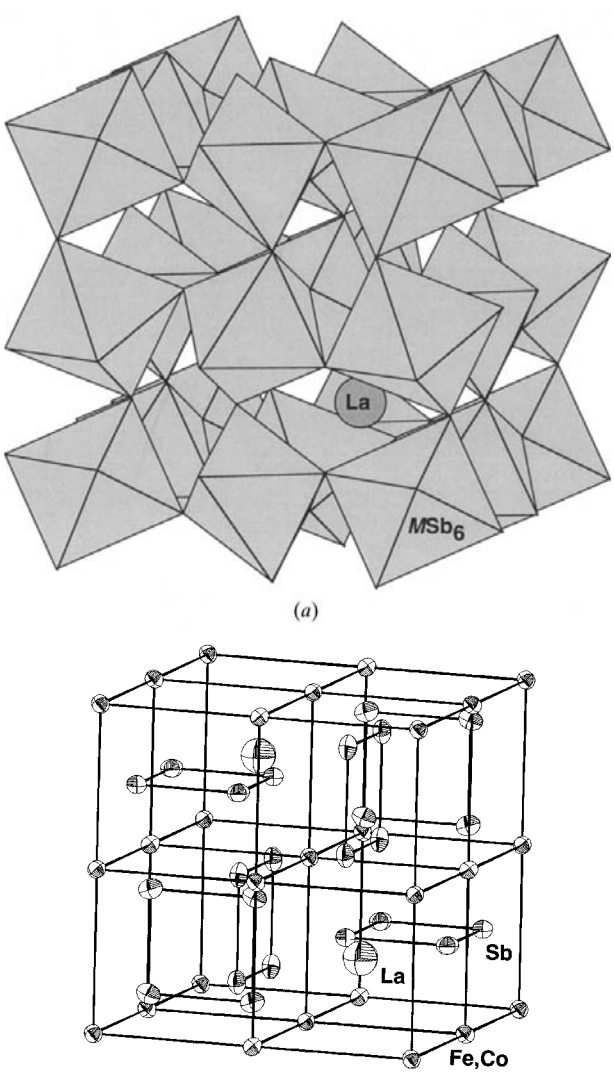

Fig. 1. (*a*) Polyhedral view of the skutterudite crystal structure. The shaded octahedra represent (Fe,Co)Sb_6, and the shaded sphere is an La atom. (*b*) *ORTEP* plot (Johnson, 1965) of $LaFe_3CoSb_{12}$, drawn with 99% probability density ellipsoids. Like near-neighbors are joined. The La atom is on a site with $m\bar{3}$ symmetry, (Fe,Co) with threefold symmetry, and Sb with mirror symmetry. For both (*a*) and (*b*) the origin has been shifted by $\frac{3}{4}, \frac{3}{4}, \frac{1}{4}$ with respect to the text description in order to illustrate the four-membered pnictogen rings.

No corrections were made for thermal diffuse scattering (TDS), but because the TDS increases with angle, neglecting this effect will only cause the ADPs to be slightly under-estimated. In this case, the under-estimation of U_{eq} as a result of neglecting the TDS can be roughly estimated by the expression developed by Willis (1969) and Schoening (1969),

$$\Delta U = (8\pi/9)(K_B T q_{max} \Psi / m V^*)[(1/v_l^2) + (2/v_t^2)],$$

where K_B is the Boltzmann constant, T is the absolute temperature, q_{max} is the radius of the spherical reciprocal lattice volume seen by the detector, $\Psi = (\theta/T)/\{(1/2) + 1/[\exp(\theta/T) - 1]\}$, θ is the Debye temperature, m is the mass of the primitive cell, $V^* = 8\pi^3/V$ is the volume of the reciprocal primitive cell, v_l is the longitudinal sound velocity, and v_t is the transverse sound velocity. The radius q_{max} was determined approximately using one half the scan width, or 1°, so that $q_{max} = 2\pi\sin(1)/\lambda$. The Debye temperature (310 K) and sound velocities (v_l = 4530 m s^{-1}, v_t = 2680 m s^{-1}) are taken

† Supplementary data for this paper are available from the IUCr electronic archives (Reference: BR0074). Services for accessing these data are described at the back of the journal.

Table 1. *Experimental details*

Chemical formula $La_{0.743}Fe_{2.74}Co_{1.26}Sb_{12}$, chemical formula weight 1791.49, cubic, $Im\bar{3}$, $Z = 2$, neutron radiation ($\lambda = 0.8387$ Å), refinement on *F*. *UCLA Crystallographic Computing Package* (Strouse, 1994) was used for data collection, cell refinement (using *LEAST*) and data reduction (using *REDUCE*).

	296 K	200 K	150 K	125 K	100 K
Crystal data					
a (Å)	9.0971 (6)	9.0854 (11)	9.0857 (11)	9.0813 (5)	9.0809 (4)
V (Å^3)	752.85	749.95	750.02	748.93	748.83
D_x (Mg m^{-3})	7.901	7.931	7.931	7.942	7.943
Data collection					
No. of measured reflections	1405	1486	1492	484	1400
No. of independent reflections	463	470	471	337	459
No. of observed reflections ($I > 0$)	321	316	318	264	330
R_{int}	0.046	0.051	0.053	0.024	0.041
Refinement					
R	0.045	0.048	0.045	0.062	0.041
wR	0.035	0.036	0.036	0.043	0.031
S	1.317	1.344	1.347	1.256	1.232
Scale factor	6.88 (4)	5.20 (2)	5.13 (2)	6.83 (4)	6.86 (3)
No. of reflections used in refinement	321	316	318	264	330
No. of parameters used	13	11	11	11	11
$(\Delta/\sigma)_{max}$	< 0.01	< 0.01	< 0.01	< 0.01	< 0.01
$\Delta\rho_{max}$ (fm Å^{-3})	1.05	0.82	1.11	0.44	0.43
$\Delta\rho_{min}$ (fm Å^{-3})	−0.48	−0.43	−0.63	−0.25	−0.42
Extinction coefficient	2.32×10^{-4}	2.2×10^{-4}	2.2×10^{-4}	2.5×10^{-4}	2.4×10^{-4}

	75 K	50 K	25 K	10 K
Crystal data				
a (Å)	9.0814 (5)	9.0839 (6)	9.0771 (4)	9.0762 (12)
V (Å^3)	748.95	749.57	747.89	747.67
D_x (Mg m^{-3})	7.942	7.935	7.953	7.955
Data collection				
No. of measured reflections	1390	1390	1362	1492
No. of independent reflections	459	459	459	472
No. of observed reflections ($I > 0$)	328	329	348	323
R_{int}	0.042	0.041	0.041	0.047
Refinement				
R	0.042	0.039	0.049	0.037
wR	0.034	0.031	0.036	0.029
S	1.359	1.245	1.390	1.159
Scale factor	6.82 (3)	6.79 (3)	6.84 (3)	5.34 (2)
No. of reflections used in refinement	328	329	348	323
No. of parameters used	11	11	11	11
$(\Delta/\sigma)_{max}$	< 0.01	< 0.01	< 0.01	< 0.01
$\Delta\rho_{max}$ (fm Å^{-3})	0.58	0.52	0.40	0.72
$\Delta\rho_{min}$ (fm Å^{-3})	−0.41	−0.46	−0.34	−0.57
Extinction coefficient	2.3×10^{-4}	2.2×10^{-4}	1.8×10^{-4}	3.1×10^{-4}

Table 2. *Fractional atomic coordinates and equivalent isotropic displacement parameters (Å^2)*

La is on site 2*a* at (0,0,0) with site occupancy 0.74 (1). Fe and Co are on site 8*c* at (1/4,1/4,1/4) with site occupancies 0.685 (8) and 0.315 (8), respectively. Sb is on site 24*g* at (0,*y*,*z*) with coordinates as given below.

T (K)	*y*	*z*
296	0.33678 (9)	0.16021 (8)
200	0.33668 (9)	0.15998 (8)
150	0.33659 (9)	0.15999 (9)
125	0.33679 (12)	0.16008 (11)
100	0.33678 (7)	0.15995 (7)
75	0.33671 (8)	0.15994 (7)
50	0.33684 (7)	0.16002 (7)
25	0.33674 (8)	0.15996 (7)
10	0.33669 (7)	0.15998 (6)

from measurements by Mandrus *et al.* (1997). When calculated by this method, the TDS contribution, ΔU = 0.0003 Å^2, is small and can be neglected.

For the room-temperature data, the Fe/Co ratio and the La-site occupation were also refined, and then fixed at these values for refinements of the lower-temperature data. Only 11 least-squares variables are needed because the atoms are all on special positions in the space group $Im\bar{3}$ (Fig. 1 and Table 2). The cell dimensions measured by the single-crystal method exhibit some scatter, but more precise cell dimensions were also determined from an aliquot of crushed crystals using the HB4 high-resolution neutron powder diffractometer (Fig. 2). Owing to restrictions on the availability of the instrument the single-crystal measurements were actually made at two different times; the two groups of measurements can be identified by their different scale factors in Table 1.

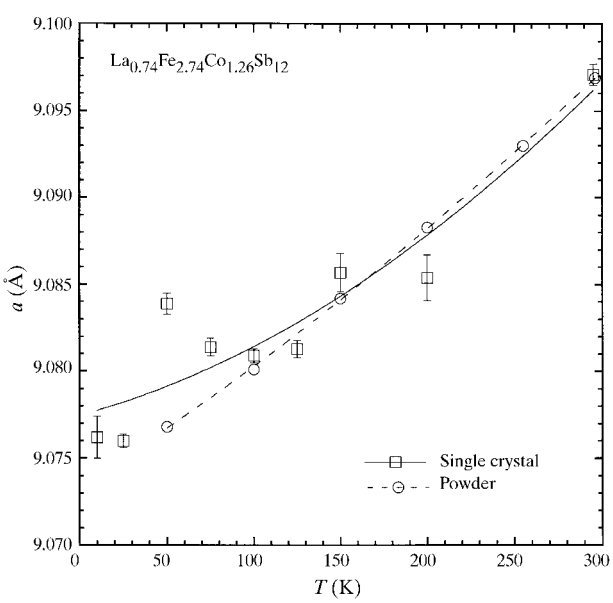

Fig. 2. Temperature dependence of the lattice parameter for the skutterudite $La_{0.74}Fe_{2.74}Co_{1.26}Sb_{12}$. 0.0213 Å was subtracted from the powder values to correct for systematic error in the wavelength determinations.

3. Results and discussion

Difference Fourier syntheses, $|F_o| - |F_c|$, for the low-temperature data do not indicate any residual density that might suggest that the La atom moves to a position away from the origin site as the crystal is cooled. Indeed, the agreements for the refinements at all temperatures are equally good. In addition, difference Fourier syntheses with the La atom removed from the model show spherically symmetrical residual scattering density at the La-atom position.

Equivalent isotropic displacement parameters U_{eq}, taken as $(1/3)TrU^{ij}$, for the (Fe,Co) and Sb atoms have typical values and are proportional to T (Fig. 3), as expected from the general form of *U(T)* (Willis & Pryor, 1975; Dunitz *et al.*, 1988). U_{eq} for La is also proportional to T, but at 296 K it is four times greater than that of (Fe,Co) and 2.7 times greater than that of Sb (Table 3). Initially, the unconstrained refinement of both the site occupation and U_{eq} for La reduced the site occupation to 0.74 (1) and U_{eq} by one half. Good scattering-length contrast allowed the Fe:Co ratio to be refined to 2.74 (3)Fe:1.26Co. The vacancies at the La site and the Fe,Co site are assumed to be randomly distributed on their respective positions. We suggest that the La-site vacancies are tied to the Co substitution to conserve the valence-electron count, because for $LaFe_4Sb_{12}$ Braun & Jeitschko (1980*a*) found the La site to be 94 (1)% occupied and earlier work (Chen *et al.*, 1997; Sales *et al.*,

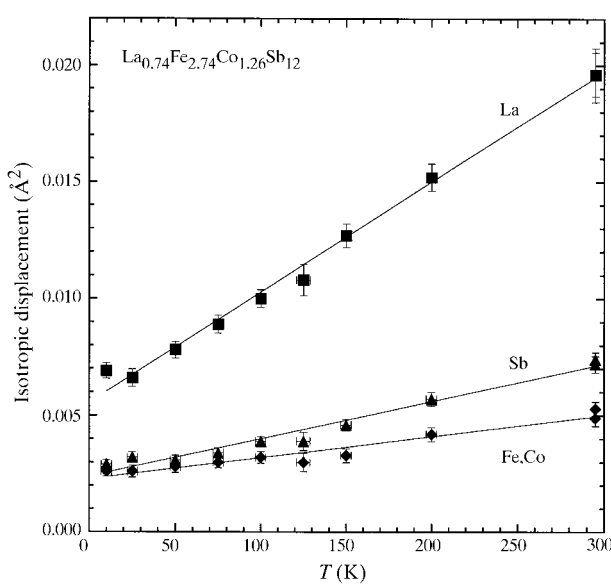

Fig. 3. Temperature dependence of the equivalent isotropic atomic displacement parameters for the skutterudite $La_{0.74}Fe_{2.74}Co_{1.26}Sb_{12}$.

Table 3. *Displacement parameters ($Å^2$)*

$$U_{eq} = (1/3)\Sigma_i\Sigma_j U^{ij} a^i a^j \mathbf{a}_i.\mathbf{a}_j.$$

	La†	Fe,Co‡		Sb§				
T (K)	$U^{11} = U_{eq}$	$U^{11} = U_{eq}$	U^{12}	U_{eq}	U^{11}	U^{22}	U^{33}	U^{23}
10	0.0069 (3)	0.0026 (1)	−0.00010 (13)	0.0029 (2)	0.00188 (19)	0.00457 (20)	0.00223 (19)	0.00040 (19)
25	0.0066 (3)	0.0026 (1)	0.00016 (15)	0.0032 (2)	0.00246 (22)	0.00488 (33)	0.00211 (22)	0.00040 (22)
50	0.0078 (3)	0.0028 (1)	0.00030 (14)	0.0031 (2)	0.00240 (20)	0.00486 (21)	0.00217 (20)	0.00037 (20)
75	0.0088 (4)	0.0030 (1)	0.00012 (15)	0.0034 (2)	0.00258 (22)	0.00524 (23)	0.00241 (22)	0.00061 (22)
100	0.0100 (3)	0.0032 (1)	0.00051 (14)	0.0039 (2)	0.00250 (19)	0.00584 (21)	0.00321 (20)	0.00054 (20)
125	0.0107 (6)	0.0030 (2)	0.00024 (28)	0.0039 (4)	0.00266 (29)	0.00581 (33)	0.00314 (31)	0.0014 (4)
150	0.0127 (5)	0.0032 (1)	0.00003 (17)	0.0046 (2)	0.00310 (25)	0.00669 (26)	0.00407 (26)	0.00019 (26)
200	0.0151 (5)	0.0042 (1)	0.00039 (18)	0.0057 (3)	0.00394 (26)	0.00830 (28)	0.00485 (26)	0.00076 (27)
296	0.0196 (9)	0.0053 (1)	0.00047 (16)	0.0074 (3)	0.00524 (25)	0.00999 (28)	0.00702 (27)	0.00126 (25)

† $U^{11} = U^{22} = U^{33}, U^{12} = U^{13} = U^{23} = 0$. ‡ $U^{11} = U^{22} = U^{33}, U^{12} = U^{13} = U^{23}$. § $U^{12} = U^{13} = 0$.

1996) showed that increasing the Co substitution shifts the resistivity from metallic to semiconducting.

The Sb position is essentially unchanged between 296 and 10 K, so the interatomic distances are given as constant fractions of the cubic cell edge. The La—Sb bond distance contracts by only 0.01 Å from 296 to 50 K, which implies that the (Fe,Co)Sb_6 framework is essentially rigid. Indeed, the comparison of the La—Sb distance, 3.3927 (9) Å, in this filled skutterudite with values observed for other lanthanum antimonides (La_2Sb, La_5Sb_3, La_4Sb_3, LaSb, $LaSb_2$) (Braun & Jeitschko, 1980*a*) shows it to be at the extreme upper limit. Note that the La—Sb distance in the filled skutterudite should actually be lengthened somewhat to correct for the large displacement of the La; at room temperature the correction amounts to 0.017 Å. The nearest neighbor Sb—Sb distances, 2.914 (1) Å, are comparable to that in Sb metal, and the (Fe,Co)—Sb distances, 2.5422 (4) Å, are intermediate between Fe or Co and Sb metal. The crystal-structure description defined by the shortest interatomic distances is that of a corner-linked octahedral framework as shown in Fig. 1(*a*). It is probably not surprising that the coefficient of linear expansion, 9×10^{-6} K^{-1}, determined from the neutron powder diffraction data is the same as that of Sb metal.

The high symmetry of each of the atom sites in skutterudite simplifies the anisotropic displacement tensors. The La site is cubic so the isotropic and anisotropic models are the same in the harmonic approximation. The Fe,Co site is on a [111]-threefold axis, and its probability density function (p.d.f.) ellipsoid is slightly elongated at room temperature, but gradually becomes essentially isotropic as the crystal is cooled to 10 K. The Sb atom is on a [100] mirror, and the principal axes of its p.d.f. ellipsoid are parallel and perpendicular to the four-membered Sb rings (Fig. 1*b*). At all temperatures, the major axis of the Sb ellipsoid is directed along the La—Sb bond. The other principal axes of the Sb ellipsoid are nearly equal, becoming more so at low temperatures, and are about one half as large as the major axis.

Difference displacement parameters evaluated along the internuclear directions between the bonded atoms can provide a measure of the atom disorder (Bürgi, 1989) and are less affected by systematic errors, such as neglecting absorption or TDS corrections (Chandrasekhar & Bürgi, 1984). The difference displacement parameter, Δ_{AB}, is evaluated along the vector between two adjacent atoms, A and B, such that

$$\Delta_{AB} = z^2_{BA} - z^2_{AB} = [\mathbf{v}]^t_{D^*}[D(U_B - U_A)D][\mathbf{v}]_{D^*},$$

where z^2_{BA} and z^2_{AB} are the respective mean-square-displacement amplitudes of B toward A and of A toward

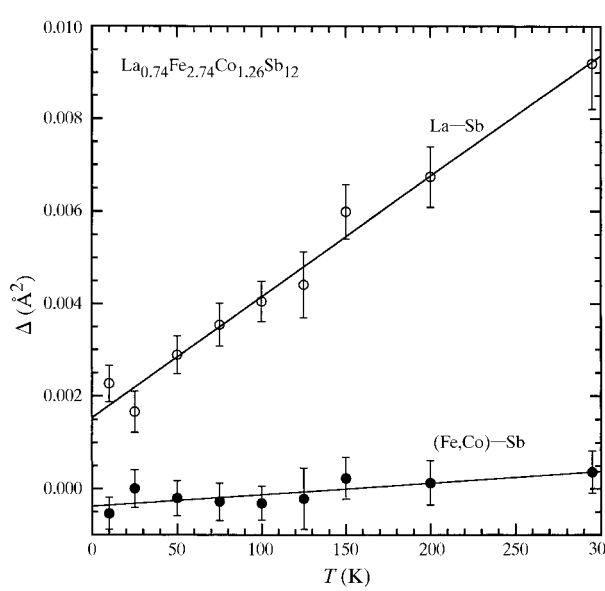

Fig. 4. Differences of atomic mean-square displacement amplitudes (Δ) measured along the bond directions at various temperatures for the skutterudite $La_{0.74}Fe_{2.74}Co_{1.26}Sb_{12}$.

Table 4. *ADP analysis results (Å²) for* $La_{0.74}Fe_{2.74}Co_{1.26}Sb_{12}$

	La	Fe,Co	Sb
$U_j^{\text{thermal}}(0)$ max.	0.0022 (2)	0.0016 (3)	0.0013 (2)
$U_j^{\text{static}}(0)$ min.	0.0037 (4)	0.0008 (3)	0.0013 (2)

B, $[\mathbf{v}]_{D^*}$ is a unit vector parallel to the AB direction defined in terms of the reciprocal basis, U_A and U_B are the respective ADP matrices for A and B, and D is a diagonal matrix containing the magnitudes of the reciprocal basis vectors. It is generally expected that for rigid atomic arrangements Δ values will be near zero (Dunitz *et al.*, 1988; Chandrasekhar & Bürgi, 1984). Fig. 4 shows the temperature dependence of Δ values evaluated along the La—Sb and (Fe,Co)—Sb directions. The $\Delta_{\text{Fe,Co}-\text{Sb}}$ values are near zero which implies that the skutterudite-type framework is essentially rigid. In contrast, the $\Delta_{\text{La}-\text{Sb}}$ values indicate a large-amplitude positional disorder or rattling-type motion of the La atom at room temperature, which diminishes upon cooling, but is still significant at low temperature. From U_{La} the r.m.s. displacement of the La atom at room temperature is 0.140 (3) Å, but the $\Delta_{\text{La}-\text{Sb}}$ value shows that with respect to the rigid skutterudite framework the r.m.s. displacement is 0.096 (1) Å. The room-temperature $\Delta_{\text{La}-\text{Sb}}$ value is large, being, for example, comparable to the effect of dynamic Jahn–Teller distortion observed in octahedrally coordinated copper complexes (Chandrasekhar & Bürgi, 1984), or to the positional disorder of H atoms in $Mg(OH)_2$ brucite (Chakoumakos *et al.*, 1997).

Further analysis is possible to separate the static positional disorder from the dynamic thermal motion. Using the inequality derived by Housley & Hess (1966),

$$U_j^2(0) \leq U_j(T)h^2/(16\pi^2 m_j K_B T), \qquad (1)$$

where h is the Planck constant, K_B is the Boltzmann constant, m_j is the the mass of atom j, and T is the temperature in K, an estimate of the maximum thermal contribution to $U(0)$ can be made by extrapolating (1) to high T where it approaches an equality; see, for example, Cheary (1991) and Argyriou (1994). The static contribution at high temperatures will be a negligible part of the ADP. Assuming that $U_j = U_j^{\text{thermal}} + U_j^{\text{static}}$, the minimum static contribution to U_j can be estimated by subtracting the maximum thermal contribution from the lowest-temperature measurement, which in this study is 10 K. When this analysis is applied, at the lowest temperature only the La site is indicated to have more static than thermal disorder whereas the other ADPs are explained by equal or less thermal vibration contributions (Table 4). Note that linear extrapolation of $U(T)$ to 0 K in this case will over-estimate the static contribution because the zero-point motion would be neglected. The static disorder is assumed to be temperature independent so it contributes 19% of the room-temperature value for the La atom. The static disorder in itself probably has contributions from a slight relaxation of the framework around the vacant La sites, but more because the real positions of the La atoms vary cell-to-cell a small amount away from their special position at the cage center. Attempts to refine a structural model with the La atom displaced from the origin toward the Sb-atom position were not stable, which supports the contention that the large La-atom displacement is principally dynamic.

For the purpose of modeling the lattice thermal conductivity, the mean nearest-neighbor separation of the La atoms in the cell is obtained from the La···La distances in the <111>, <100>, and <110> directions. This mean value at room temperature is 7.5 Å, and corresponds to the mean free path of vibrations used to correctly estimate the measured lattice thermal conductivity (Mandrus *et al.*, 1997; Sales *et al.*, 1997).

4. Conclusions

Neutron diffraction data confirm the large mean-square displacement of the La atom in a filled skutterudite antimonide and analysis of its temperature dependence identifies a significant temperature-independent component ascribed to static disorder, amounting to 19% of the room-temperature value. Site-occupancy refinements clearly show 25% vacancies on the La site and an Fe:Co ratio of 2.74 (3)Fe:1.26Co. This study reenforces the picture of the filled skutterudites as being rigid frameworks with the lanthanide atoms occupying oversized atomic cages, and is consistent with the overly long La—Sb distances and relatively small coefficient of linear expansion, $9 \times 10^{-6}\,\text{K}^{-1}$. The large-amplitude rattling of the La atom can be effectively linked to the dramatic decrease of the lattice contribution to the thermal conductivity (Keppens *et al.*, 1998; Sales *et al.*, 1998), which is a key factor in improving the thermoelectric behavior of clathrate-like materials (Nolas *et al.*, 1996). In a recent study of the effect of partial filling on the lattice thermal conductivity of skutterudites, Nolas *et al.* (1998) observed that a small concentration of La filling results in a large decrease in the lattice thermal conductivity. Moreover, the decrease in the lattice thermal conductivity saturates at an intermediate filling, which is consistent with the expected behavior of the ADP upon filling (Sales *et al.*, 1999). For other filled skutterudites such as $CaFe_4Sb_{12}$, $NdFe_4Sb_{12}$, and $NdOs_4Sb_{12}$ (Evers *et al.*, 1994, 1995), for which the ADPs of the filling atom are even larger than those reported here, we predict that their lattice thermal conductivities will be even lower. This structure–property relationship, *i.e.*, thermal conductivity from ADPs, provides a new paradigm for the exploration of thermoelectric materials.

Sincere thanks go to Carroll Johnson and Michael Burnett for help with the diffractometer control system. Oak Ridge National Laboratory is managed by Lockheed Martin Energy Research Corporation for the US Department of Energy under contract number DE-AC05-96OR22464.

References

Argyriou, D. N. (1994). *J. Appl. Cryst.* **27**, 155–158.
Braun, D. J. & Jeitschko, W. (1980*a*). *J. Less Common Met.* **72**, 147–156.
Braun, D. J. & Jeitschko, W. (1980*b*). *J. Solid State Chem.* **32**, 357–363.
Braun, D. J. & Jeitschko, W. (1980*c*). *J. Less Common Met.* **76**, 33–40.
Bürgi, H. B. (1989). *Acta Cryst.* B**45**, 383–390.
Chakoumakos, B. C., Loong, C.-K. & Schultz, A. J. (1997). *J. Phys. Chem. B*, **101**, 9458–9462.
Chandrasekhar, K. & Bürgi, H. B. (1984). *Acta Cryst.* B**40**, 387–397.
Cheary, R. W. (1991). *Acta Cryst.* B**47**, 325–333.
Chen, B., Xu, J. H., Uher, C., Morelli, D. T., Meisner, G. P., Fleurial, J. P., Caillat, T. & Borshchevsky, A. (1997). *Phys. Rev. B*, **55**, 1476–1480.
Dunitz, J. D., Schomaker, V. & Trueblood, K. N. (1988). *J. Phys. Chem.* **92**, 856–867.
Evers, B. H. C., Boonk, L. & Jeitschko, W. (1994). *Z. Anorg. Allg. Chem.* **620**, 1028–1032.
Evers, B. H. C., Jeitschko, W., Boonk, L., Braun, D. J., Ebel, T. & Scholz, U. D. (1995) *J. Alloys Compd.* **224**, 184–189.
Housley, R. M. & Hess, F. (1966). *Phys. Rev.* **146**, 517–526.
Johnson, C. K. (1965). *ORTEP.* Report ORNL-3794. Oak Ridge National Laboratory, Tennessee, USA.
Keppens, V., Mandrus, D., Sales, B. C., Chakoumakos, B. C., Dai, P., Coldea, R., Maples, M. B., Gajewski, D. A., Freeman, E. J. & Bennington, S. (1998). *Nature*, **395**, 876–878.
Larson, A. C. & Von Dreele, R. B. (1986). *GSAS. Generalized Structural Analysis System.* Report LAUR-86-748. Los Alamos National Laboratory, Los Alamos, New Mexico, USA.
Mahan, G. D., Sales, B. C. & Sharp, J. (1997). *Phys. Today*, **50**, 42–47.
Mandrus, D., Sales, B. C., Keppens, V., Chakoumakos, B. C., Dai, P., Boatner, L. A., Williams, R. K., Thompson, J. R., Darling, T. W., Migliori, A., Maple, M. B., Gajewski, D. A. & Freeman, E. J. (1997). *Thermoelectric Materials – New Directions and Approaches*, edited by T. M. Tritt, G. Mahan, H. B. Lyon Jr and M. G. Kanatzidis, pp. 199–209. Pittsburgh: Materials Research Society.
Morelli, D. T. & Meisner, G. P. (1995). *J. Appl. Phys.* **77**, 3777–3781.
Nolas, G. S., Cohn, J. L. & Slack, G. A. (1998). *Phys. Rev. B*, **58**, 164–170.
Nolas, G. S., Slack, G. A., Morelli, D. T., Tritt, T. M. & Ehrlich, A. C. (1996). *J. Appl. Phys.* **79**, 4002–4008.
Sales, B. C., Chakoumakos, B. C. & Mandrus, D. (1999). In preparation.
Sales, B. C., Chakoumakos, B. C., Mandrus, D., Sharp, J. W., Dilley, N. R. & Maple, M. B. (1998). In *Thermoelectric Materials – The Next Generation Materials for Small-Scale Refrigeration and Power Generation Applications*, edited by T. M. Tritt, G. Mahan, H. B. Lyon Jr & M. G. Kanatzidis. Materials Research Society Symposium Proceedings. In the press. Pittsburgh: Materials Research Society.
Sales, B. C., Mandrus, D., Chakoumakos, B. C., Keppens, V. & Thompson, J. R. (1997). *Phys. Rev. B*, **56**, 15081–15089.
Sales, B. C., Mandrus, D. & Williams, R. K. (1996). *Science*, **272**, 1325–1328.
Schoening, F. R. L. (1969). *Acta Cryst.* A**25**, 484–486.
Sears, V. F. (1992). *Neutron News*, **3**, 26–37.
Slack, G. A. (1995). *Thermoelectric Handbook*, edited by D. M. Rowe, p. 407. Boca Raton, Florida: CRC.
Strouse, C. (1994). Personal communication.
Willis, B. T. M. (1969). *Acta Cryst.* A**25**, 277–300.
Willis, B. T. M. & Pryor, A. W. (1975). *Thermal Vibrations in Crystallography.* Cambridge University Press.